Geomechanics and Engineering, *Vol. 38, No. 6 (2024) 571-581*
https://doi.org/10.12989/gae.2024.38.6.571

Discrete element numerical analysis for simulating trapdoor tests to assess loosening earth pressure on tunnel linings

Chaemin Hwang[1a], Junhyuk Choi[2b], Jee-Hee Jung[3c] and Hangseok Choi*[1]

[1]*School of Civil, Environmental and Architectural Civil Engineering, Korea University, 145, Anam-ro, Seongbuk-gu, Seoul, Republic of Korea*
[2]*Civil Overseas Engineering Team, Daewoo Engineering & Construction Co., Ltd., 170, Eulji-ro, Jung-gu, Seoul, Republic of Korea*
[3]*Korea Expressway Corporation Research Institute, 24, Dongtansunhwan-daero 17-gil, Hwaseong-si, Gyeonggi-do, Republic of Korea*

(*Received November 23, 2023, Revised February 7, 2024, Accepted February 23, 2024*)

Abstract. Concrete linings in tunnels constructed by drilling and blasting such as NATM serve as a secondary support structure. However, these linings can face unexpected earth pressures if the primary support deteriorates or if ground conditions become unfavorable. It is crucial to determine the loosening earth pressure that allows the lining to maintain its structural integrity and prevent damage caused by this pressure. This study proposes a numerical model for simulating the trapdoor test and developing a method for calculating the loosening earth pressure. The discrete element method (DEM) was employed to describe the soil characteristics around the tunnel. Using this numerical model, a sequence of experimental trapdoor steps was simulated, and the loosening earth pressure was analyzed. Contact parameters were calibrated based on an analysis of a triaxial compression test. The reliability of the developed model was confirmed through a comparison between simulation results and laboratory test findings. The model was used to calculate the contact force applied to the trapdoor plate and to assess the settlement of soil particles. Furthermore, the model accounted for the soil-arching effect, which effectively redistributes the load to the surrounding areas. The proposed model can be applied to analyze the tunnel's cross-sectional dimensions and design stability under various ground conditions.

Keywords: discrete element method; loosening earth pressure; soil-arching effect; trapdoor test

1. Introduction

The stability of tunnels constructed by drilling and blasting such as NATM is critical and relies on a combination of support systems. Primary support structures, including sprayed concrete and rock bolts, play a vital role in enhancing the mechanical stability of a tunnel during excavation and operation. Meanwhile, secondary support systems, such as concrete linings, ensure the tunnel's continued serviceability. However, unforeseen factors such as primary support deterioration, adverse ground conditions, and other unpredictable events can exert unexpected pressures on the lining. This can result in convergence displacement or damage during construction and operation. Calculating the loosening earth pressure is essential in designing the lining to mitigate these risks.

Numerous studies have aimed to provide accurate estimates of ground loosening earth pressure on concrete linings. Typically, two approaches are employed to assess loosening earth pressure: the theoretical method, which involves an equation considering various mechanical factors, and the empirical method, which is based on Terzaghi's rock load classification and rock mass rating (RMR). However, these approaches come with distinct definitions of loosening earth pressure and often fail to account for critical factors, such as tunnel cross-section and surrounding ground conditions. Consequently, current criteria for concrete lining design tend to overestimate loosening earth pressure, leading to uneconomical tunnel construction practices.

To address the challenge of overdesigning tunnel linings, various numerical approaches have been proposed. Numerical methods enable the assessment of loosening earth pressures while considering factors such as the tunnel's cross-sectional geometry, soil conditions, and geometric nonlinearities. Additionally, these methods allow for the simultaneous evaluation of ground earth pressures and deformations, and they can simulate the tunnel's construction phases. Seo *et al*. (2002) proposed a numerical model for ground-lining interaction that comprehensively represents the entire tunnel excavation process, including the loss of primary support strength, by employing a mass-spring coupling approach. Zhao *et al*. (2017) conducted a comparative study between commonly used analytical calculation methods in lining design and numerical methods. They explored the feasibility of incorporating realistic tunneling process factors into the numerical model.

*Corresponding author, Professor
E-mail: hchoi2@korea.ac.kr
[a]Ph.D. Student
[b]Staff
[c]Senior Researcher

ISSN: 2005-307X (Print), 2092-6219 (Online)

Su *et al*. (2022) developed a refined numerical model for shield TBM segment linings based on the load-structure method. This model incorporates detailed lining components such as reinforcement and connecting bolts and is capable of analyzing the internal forces and transverse deformations of the segment linings within the soil loosening zone.

In the past decade, several approaches have been proposed for calculating loosening earth pressure on tunnel linings, and a trapdoor experiment has emerged as a novel method for simulating underground tunneling, since Terzaghi (1943) first introduced. The trapdoor test involves creating a void space in the soil, allowing for the observation of settlement behavior of soil particles and soil-arching effect. The soil-arching effect, which entails the transfer of contact forces from the failure area to the surrounding soil mass, is a phenomenon that can be observed in ground composed of granular soil particles. In tunneling, soil arching occurs when soil particles move inward to the center of an underground space due to ground excavation. Various studies aimed at estimating the soil-arching effect have been developed based on trapdoor tests (Murayama and Matsuoka 1971, Evans 1983, Wu *et al*. 2004, Moradi and Abbasnejad 2015, Han *et al*. 2017, Song *et al*. 2018, Liang *et al.* 2020).

In addition, the concept of the loosening zone can also be explored through trapdoor tests. During tunneling, the loosening zone exists above the excavated ground, where soil stress is redistributed, and soil particles are rearranged due to the soil-arching effect (Hong and Kim 2014). Terzaghi (1943) initially identified this loosening zone using a trapdoor model that lowered the floor plate, leading to plastic deformation of the soil. Ladanyi and Hoyaux (1969) performed trapdoor experiments employing a mechanical analog model of a granular mass to study the mechanism of mass displacement. McNulty (1965) proposed a ground-arching ratio as a means to estimate load transfer from the loosening zone.

Building upon this research background, this study aims to develop a numerical model for estimating the loosening earth pressure exerted on tunnel linings by numerically simulating trapdoor tests. Various numerical analysis techniques have been used to create a numerical trapdoor model. Discontinuous deformation analysis (DDA) has been used to investigate the mechanical behavior of inclined jointed rock masses during excavation (Wu *et al*., 2004) and predict mining-induced slope settlement in inclined cemented rock formations (Do *et al*. 2017). Trapdoor studies using the finite element method (FEM) have also been conducted to calculate the failure load based on trapdoor geometries and soil properties (Koutsabeloulis and Griffiths 1989) and to assess the soil-arching effect (Pardo and Sáez 2014). However, these FEM models fail to describe post-failure phenomena such as severe grain rearrangement, sliding, crushing, and rolling (Tu *et al*. 2017). Therefore, simulating soil particle movement in trapdoor experiments with FEM is challenging due to the intricate interaction between ground stress redistribution and soil particle rearrangement induced by tunnel excavation. This complexity makes it challenging to accurately capture the soil-arching effect and estimate the precise loosening zone.

To determine the loosening earth pressure through numerical analysis of the trapdoor, employing the discrete element method (DEM) is an appropriate choice. In the DEM model, the component particles are treated as rigid bodies with finite stiffness. The model operates through three key calculation steps: internal force evaluation for the calculation of contact forces, equation of motion integration to analyze element displacements, and contact detection for identifying contacts and eliminating broken contacts (Tavarez and Plesha 2007). The DEM can physically describe the behavior of particulate materials and simulate the deformation and discontinuous processes of discrete particle formations in dynamic conditions, making it a suitable alternative to FEM for analyzing soil failure problems (Jiang *et al*. 2012). DEM, initially proposed by Kundal and Strack (1979), has found applications in geotechnical engineering with investigating the behavior of granular and discrete media such as soils and rocks (Jiang *et al*. 2012, Shen *et al*. 2016, Liakas *et al*. 2017, Zhu *et al.* 2017, Shang 2020, Sarfarazi and Tabaroei 2020). Consequently, employing a DEM, which can numerically simulate the movement of numerous particles under substantial deformation, is crucial for analyzing trapdoor experiments that induce ground deformation.

Prior to conducting DEM modeling, micro-mechanical parameters (i.e., contact parameters) must be calibrated to facilitate the application of macroscopic parameters such as Druker-Prager, Mohr-Coulomb, and modified Cam-Clay parameters (Fakhimi *et al*. 2002, Lee *et al*. 2021). In geotechnical engineering, the microscopic parameters are typically determined through preliminary numerical analyses simulating various shear strength tests (Cho *et al*. 2007, Chen *et al*. 2011, Yang *et al*. 2018, Hu *et al*. 2020, Choi *et al*. 2020, Xu *et al*. 2020, Zhou *et al.* 2023).

This study introduces a numerical model for trapdoor simulations to estimate the reliable loosening earth pressure to optimize tunnel lining design. DEM is employed to analyze the plastic behavior of soil particles due to excavation and to estimate the loosening zone. Initially, a DEM analysis of the triaxial compression test was conducted to calibrate the microscopic parameters of the soil particles. The calibration model validated the Mohr-Coulomb parameters using experimental results, and the optimized contact parameters thus determined were subsequently applied to the trapdoor model. The numerical model, simulating the trapdoor test process as conducted by Jung (2009), characterizes the behavior and stress distribution of the surrounding soil. Additionally, it assesses the loosening zone generated by plastic deformation of discrete soil particles and computes the earth pressure exerted on the trapdoor. These calculations include assessing the influence of contact parameters on the cover depth. All computations within this model were executed using a three-dimensional particle flow code (PFC3D).

2. Laboratory trapdoor test

2.1 Test apparatus setup

Laboratory trapdoor experiments were performed to observe soil deformation behavior during NATM tunneling.

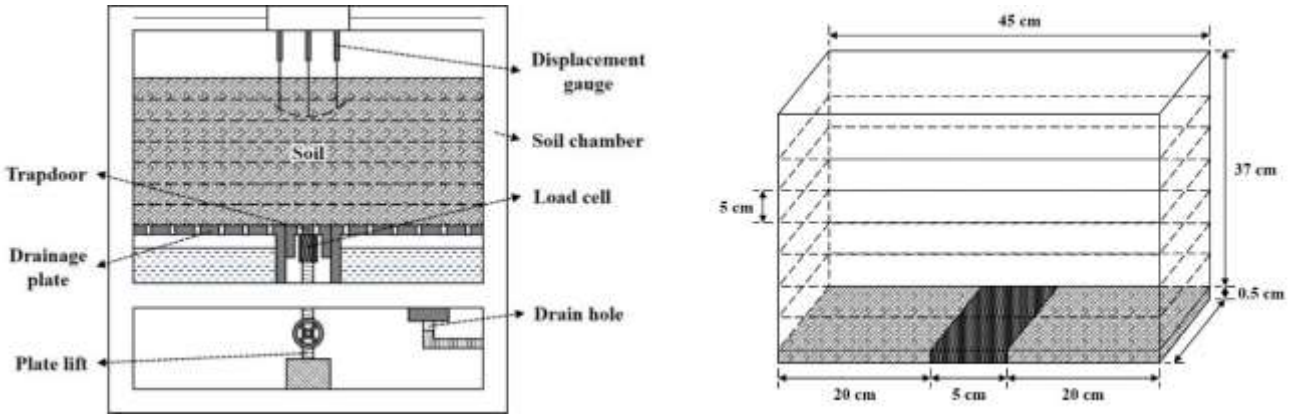

(a) Schematic of the trapdoor test apparatus (b) Schematic of the trapdoor soil chamber

Fig. 1 Configuration of a laboratory trapdoor test setup

The experimental setup consisted of a soil chamber and a trapdoor plate. The inner walls of the chamber were made of reinforced glass to minimize any impact of wall friction on soil behavior. To reduce friction during the movement of the trapdoor plate, both the trapdoor and drain plates were made thinner. The trapdoor plate, positioned at the center of the chamber floor, moved downward at a fixed velocity using screw pistons to induce soil deformation. The earth pressure exerted on the trapdoor plate was measured, while a strain gauge positioned above the soil specimen monitored surface settlement. Fig. 1 shows a schematic of the test apparatus setup and soil chamber.

Once the soil specimen was prepared in the chamber, trapdoor experiments were conducted by lowering the trapdoor plate by 5 mm to induce ground deformation. During the experiment, after every 5 mm movement of the trapdoor plate, the specimen was allowed to stabilize for 5 minutes, during which both earth pressure and surface displacement were measured. This process was repeated ten times, allowing for the observation of stress redistribution within the soil specimen through the measurement of pressure exerted on the trapdoor plate.

2.2 Soil specimen

In the laboratory trapdoor test, Jumunjin sand, a standard sand commonly used in Korea, was chosen as the test material with 0% water content to ensure low cohesion. Table 1 summarizes the basic physical properties of the Jumunjin sand. In addition, Fig. 2 shows the grain size distribution of the soil specimen.

The Jumunjin sand was prepared to a relative density of 98.9% using the sand raining method. No consideration of drainage conditions was made because the specimens were oven-dried. For better visual observation of soil behavior as the trapdoor plate lowered, a thin layer of black sand was evenly distributed within the sand specimen at 5 cm intervals.

2.3 Test results

The results of the laboratory trapdoor test revealed the displacement of the soil specimen within the chamber as the trapdoor plate moved downward, as depicted in Fig. 3(a).

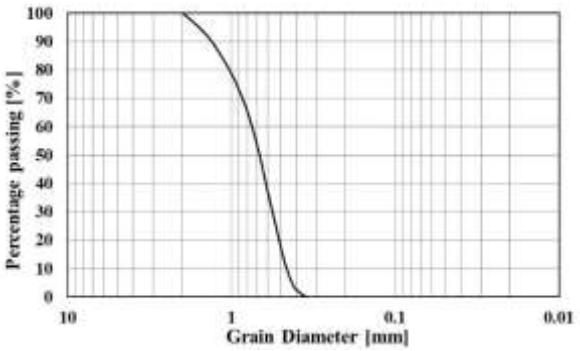

Fig. 2 Grain-size distribution curve of Jumunjin sand

Table 1 Soil properties used for laboratory trapdoor test

Property	Value
USCS	SP
Specific gravity, G_s	2.626
Coefficient of uniformity, C_u	1.630
Coefficient of curvature, C_c	0.877
Minimum void ratio, e_{min}	0.579
Maximum void ratio, e_{max}	0.851

The displacement of all soil specimens was visually assessed using the black sand layers placed within the chamber. All soil above the trapdoor plate exhibited plastic deformation, leading to surface settlement. In other words, the shallow soil cover depth did not provide sufficient space for the transfer of earth pressure into the surrounding ground. Consequently, surface settlement could not be prevented, and accurate estimation of the loosening zone was not possible.

In addition, the study measured the pressures on the trapdoor plate at each stage of trapdoor's movement to analyze changes in earth pressure. The pressure trends are illustrated in Fig. 3(b). The x- and y-axes represent the

(a) Soil deformation

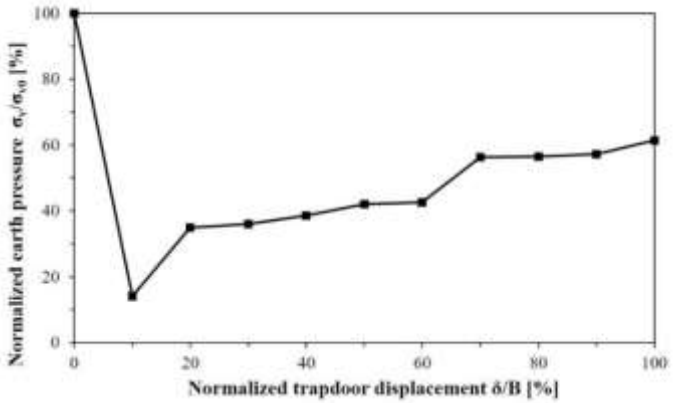

(b) Behavior of earth pressure according to the trapdoor displacement

Fig. 3 Laboratory trapdoor test results

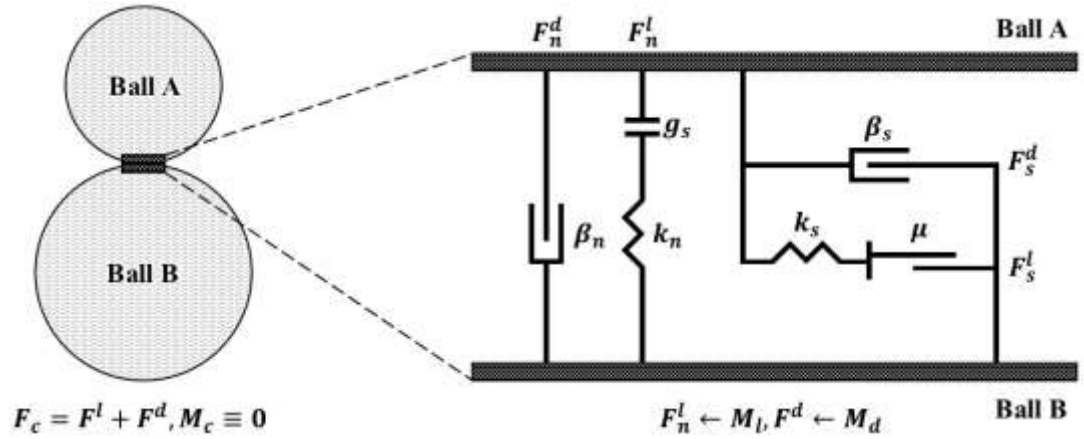

(a) Schematic of the model with two elements (b) Configuration of contact force and contact moment

Fig. 4 Analysis layout of the linear contact model

trapdoor's downward displacement normalized to the trapdoor's width and the earth pressure normalized to the initial pressure at each stage, respectively. Initially, the vertical earth pressure decreased rapidly during the first 5 mm of the trapdoor plate's movement, and then gradually increased as the experiment progressed. This suggests that the trapdoor initially only experienced a portion of the earth pressure due to the soil-arching effect as it began to deform the ground. However, as the trapdoor's displacement increased, the soil-arching structure weakened, leading to a gradual increase in earth pressure. The results showed that when the trapdoor was lowered by 50 mm, the normalized earth pressure on the plate increased by 47.2% from the minimum pressure, reaching 61.3%.

3. DEM numerical modeling

3.1 Particle flow simulation

To simulate the trapdoor experiment, this study adopted the Discrete Element Method (DEM) with a commercial numerical program known as the three-dimensional particle flow code (PFC3D). The linear contact model, which is a built-in feature in PFC3D, was applied to characterize the behavior of low-cohesion sand, as observed in the laboratory trapdoor tests. The linear model excludes relative rotational resistance while allowing for slip by constraining the shear force to the Coulomb limit.

Fig. 4 shows a schematic representation of the linear contact model. The contact force (F_c) is divided into two components: dashpot force (F^d) and linear force (F^l), that is $F_c = F^d + F^l$. Importantly, there is no contact moment (M_c), as depicted in Fig. 4(a). The contact force is determined by the governing contact parameters, including the effective modulus (E^*), friction coefficient (μ), normal stiffness (k_n), shear stiffness (k_s), normal critical damping ratio (β_n), and shear critical damping ratio (β_s), as shown in Fig. 4(b). These parameters were calibrated before their application in the proposed model.

3.2 Calibration of particle contact properties

In contrast to other numerical analysis methods, determining the soil parameters, such as internal friction angle and cohesion, for initializing the DEM model is a

Table 2 Dimensions of the triaxial compression test model

Property	Value
Size of specimen, D × H [mm]	70 × 140
Confining pressure [kPa]	50, 100, 150
Strain rate [mm/min]	0.00102
Density of ball element [kg/m^3]	2700
Number of ball elements	2346
Elastic modulus of shell element [kPa]	500
Thickness of shell element [mm]	6
Density of shell element [kg/ m^3]	90

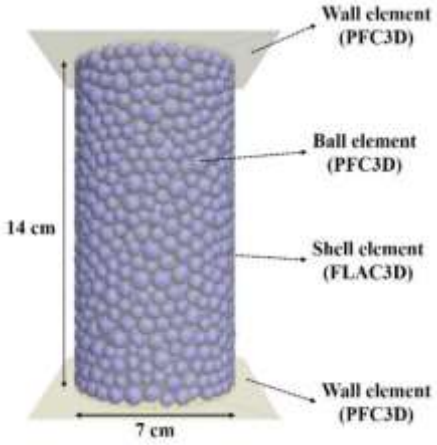

Fig. 5 Geometry of the triaxial compression test model for calibrating contact parameters

complex process. Therefore, a calibration process was carried out to determine these parameters before the trapdoor simulation. To apply the calibration results to the trapdoor model, laboratory triaxial compression tests were conducted by Jung (2009), and their outcomes were compared with the results from the numerical triaxial compression model.

A fully saturated triaxial compression test was conducted on the same Jumunjin specimen used in the trapdoor test. The Mohr-Coulomb strength parameters were determined with an internal friction angle of 40° and a cohesion value of 0 kPa (Jung 2009). These parameters served as the target values for the parameters estimated by the calibration model.

Table 2 provides a comprehensive overview of the numerical properties involved in the calibration process. The specimen scale (diameter: 70 mm; height: 140 mm) and ball element size were determined, and shell elements available in another commercial numerical code of FLAC3D were placed around them. During the analysis, these shell elements acted as a membrane, transmitting the confining pressure to the ball element. Various confining pressures (50, 100, and 150 kPa) and a constant strain rate (0.00102 mm/min) were applied, each corresponding to specific calibrations in this study. The model geometry, as shown in Fig. 5, was configured, and numerical analysis was conducted by applying a load to the upper wall element.

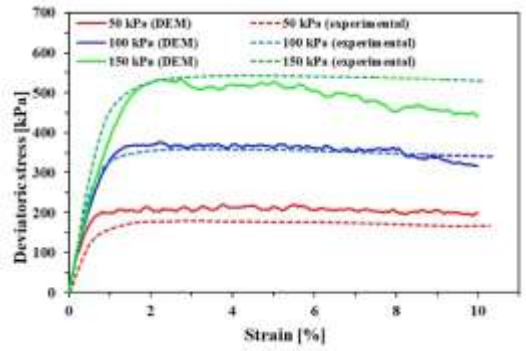

(a) Stress-strain curve

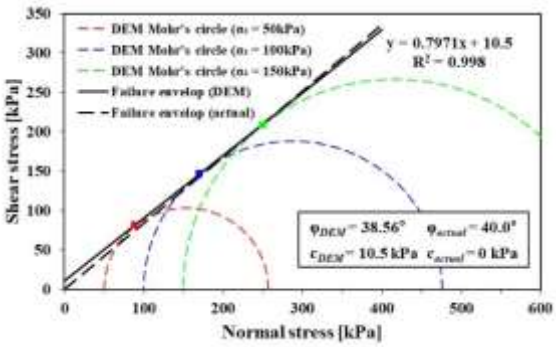

(b) Mohr–Coulomb failure envelope

Fig. 6 Results of triaxial compression tests for the calibration of contact properties

Iterative calibration was performed by adjusting various parameters until the desired Mohr–Coulomb strength parameters, such as internal friction angle and cohesion, matched the Mohr–Coulomb failure envelopes. Fig. 6 displays the calibration results of the contact parameters obtained using the triaxial compression test model. The contact parameters of the calibration model were optimized to ensure that the simulation results align with those obtained from the laboratory tests conducted under three different confining pressures, as illustrated in Fig. 6(a). Fig. 6(b) illustrates the calibrated Mohr–Coulomb strength parameters compared with the target parameters: internal friction angle = 38.56° and cohesion = 10.5 kPa. Table 3 outlines the contact parameters determined for the calibration.

3.3 Development of DEM numerical model

The numerical model for the trapdoor test was developed using DEM with calibrated contact parameters. This model simulated a soil chamber with wall elements of the identical dimensions (length: 45 cm, width: 15 cm) to those used in the laboratory tests. A trapdoor plate was positioned in the center of the chamber floor, capable of moving downward to induce displacement of the ball elements in the chamber. Fig. 7 illustrates the overall geometry of the trapdoor test model. In addition, several parameters were configured for model development, as detailed in Table 4. To minimize the friction effect from the inner walls of the chamber, the friction coefficient between the ball-wall elements was set to 0.1.

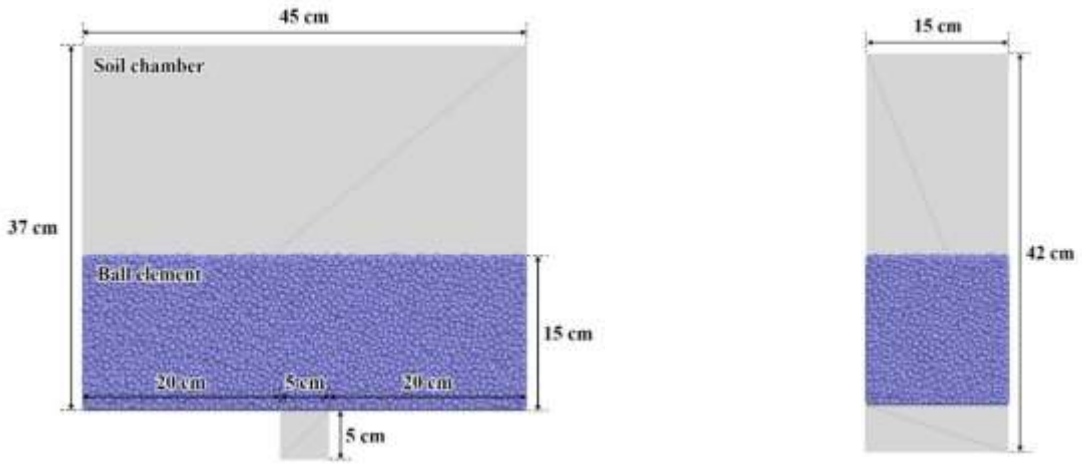

(a) Front view (b) Side view

Fig. 7 DEM model of the trapdoor test

Table 3 Calibrated properties after triaxial compression test

Contact property	Calibrated value
Effective modulus, E [kN/m^2]	90000
Friction coefficient, μ	0.49
Normal stiffness, k_n [kN/m]	70
Shear stiffness, k_s [kN/m]	70
Normal critical damping ratio, β_n	0.04
Shear critical damping ratio, β_s	0.04

Table 4 Contact parameters between ball-wall elements

Contact parameter	Value
Friction coefficient	0.1
Normal stiffness [N/m]	100
Shear stiffness [N/m]	100
Normal critical damping ratio	0.1

Following the trapdoor test procedure, the proposed model was used to estimate the loosening earth pressure exerted on the tunnel linings. Once the soil particles were established and stabilized, the trapdoor plate was incrementally lowered by 5 mm at each step. The model analysis was conducted ten times, with measuring particle displacement and earth pressure exerted on the trapdoor plate. This study evaluated the loosening earth pressure and development of the soil-arching effect around the tunnel lining.

3.4 Discussion of model test results

The DEM model of the trapdoor experiment was used to assess the loosening earth pressure and displacement distribution resulting from ground deformation. Initially, the vertical earth pressure was calculated for each downward movement of the trapdoor plate and validated using laboratory experiment results. Fig. 8 shows that the DEM

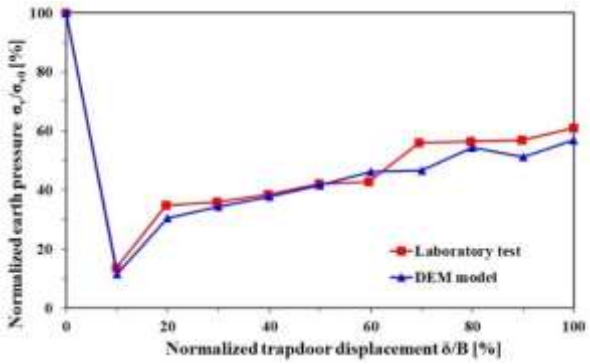

Fig. 8 Comparison of results between the DEM model and laboratory test of the trapdoor test

model yielded pressure curves closely similar to those observed in the laboratory experiment. The normalized earth pressure derived from DEM decreased by 11.7% during the initial downward movement and then gradually increased to 52.7%. At a 20% normalized trapdoor displacement, the difference between the DEM model and laboratory experiment reached a peak of 20.0%, while it decreased to a minimum of 1.75% at 80%.

Fig. 9 displays the vertical displacement distribution of the soil particles at each stage of the trapdoor plate movement, which was obtained from the DEM model. During the trapdoor test simulation, soil elements with displacements exceeding 5 mm were classified as plastically deformed soil, defining the loosening zone. At the early stage of the trapdoor simulation, the trapdoor movement induced soil deformation near the chamber's bottom. However, not all of the soil above the trapdoor plate underwent plastic deformation due to the formation of soil arching around the loosening zone, leading to stress redistribution. As a result, no surface settlement occurred until Stage 6.

From Stage 7, the loosening zone began extending toward the ground surface, causing a gradual increase in surface settlement. The soil cover depth proved insufficient

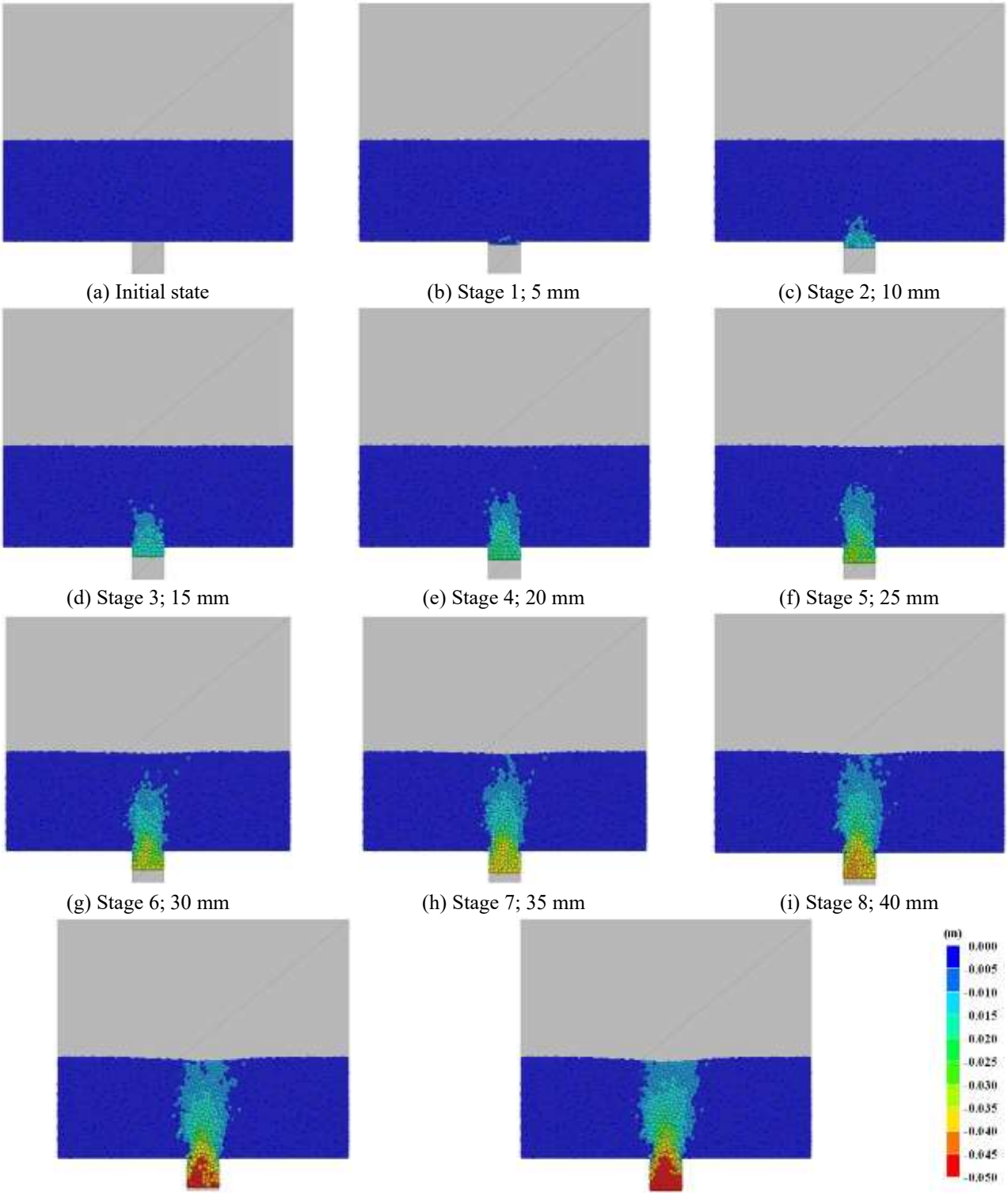

(a) Initial state (b) Stage 1; 5 mm (c) Stage 2; 10 mm

(d) Stage 3; 15 mm (e) Stage 4; 20 mm (f) Stage 5; 25 mm

(g) Stage 6; 30 mm (h) Stage 7; 35 mm (i) Stage 8; 40 mm

(j) Stage 9; 45 mm (k) Stage 10; 50 mm

Fig. 9 Particle displacement at each stage of trapdoor downward movement

enough for transferring contact forces, preventing the development of the soil-arching effect. Accordingly, all soil above the trapdoor plate was plastically deformed at the end of the trapdoor simulation.

4. Loosening zone around a tunnel

In this study, DEM numerical simulations for trapdoor tests were performed at different soil cover depths (150,

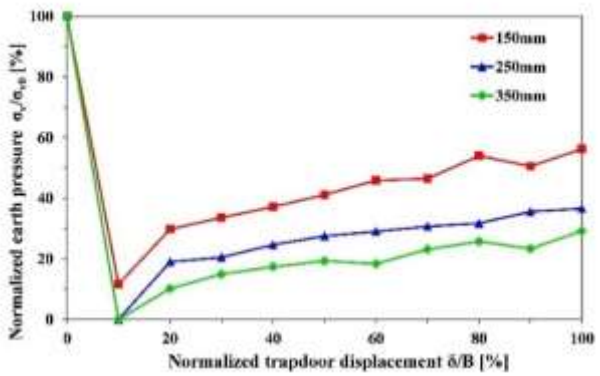

Fig. 10 Effect of cover depth on normalized earth pressure

250, and 350 mm) to accurately estimate the loosening zone, as shown in Fig. 10. When the trapdoor plate was initially lowered, the earth pressure on the trapdoor in the other two models (with cover depths of 250 and 350 mm) was significantly lower than that in the model with a 150 mm cover depth. Subsequent analysis reveals that the model with greater cover depth exhibited a lower normalized earth pressure on the trapdoor. This observation suggested that soil-arching became more evident at greater cover depths.

This study also calculated both the initial and final contact forces on the trapdoor plate at the three soil cover depths to investigate the effect of this cover depth and estimate the height of the loosening zone in the ground. Table 5 and Fig. 11 present a summary of the analysis results. As shown in Fig. 11(a), the initial contact force exhibited a linear increase ($R^2 = 0.9985$) with the soil cover depth. In contrast, the final contact force demonstrated an almost linear increase pattern, albeit with a smaller R^2 value compared to the initial contact force, as depicted in Fig. 11(b). However, for the loosening zone height, no linear relationship with the soil cover depth was observed; the R^2 value was very low, as shown in Fig. 11(c). Consequently, beyond a specific point, the loosening zone height appeared to be no longer influenced by the soil cover depth. In other words, when the soil cover depth exceeded a certain height, the loosening zone formed into a complete elliptical shape. Beyond this zone, stress transfer and particle rearrangement took place due to the soil-arching effect, resulting in the self-stabilization of the ground, as discussed by Hong and Kim (2014). Consequently, the height of the loosening zone ceased to expand further. This finding aligns with Terzaghi's suggestion (1943), which indicates that the thickness of the loosening zone is primarily influenced by the tunnel width rather than the soil cover depth.

Fig. 12 shows a detailed representation of the loosening zones for each soil cover depth in the numerical models. In Fig. 12(a), insufficient ground height led to the extension of the loosening zone to the surface, resulting in surface settlement. Conversely, in the other two models, the loosening zone formed an elliptical shape with no extension to the surface, as depicted in Figs. 12(b) and 12(c). This elliptical shape may indicate the development of soil-

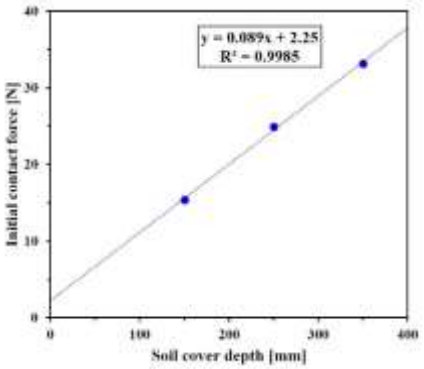

(a) Initial contact force

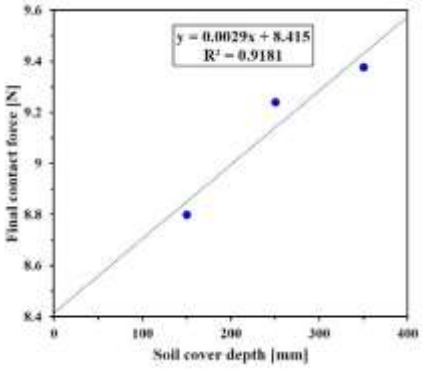

(b) Final contact force

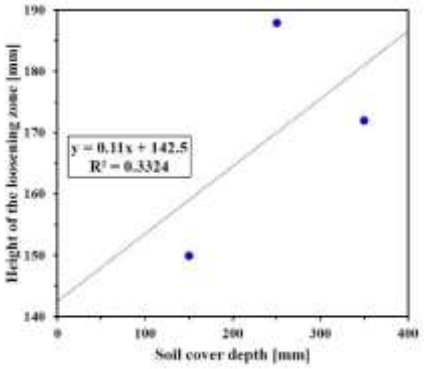

(c) Height of the loosening zone

Fig. 11 Correlation between soil cover depth and trapdoor model analysis results

arching with contact force transfer occurring in the direction of arch formation. In addition, both loosening zones exhibited similar heights, and their widths did not surpass the width of the trapdoor plate. Hence, it appears that the soil cover depth did not exert a significant influence on the size of the loosening zone.

The adoption of the proposed numerical model, as an alternative to the conventional empirical method that often results in the overdesign of lining thickness and reinforcement, enables more economical construction, improved tunnel constructability, and enhanced serviceability during the operation phase. Furthermore, this study on the loosening zone in relation to soil cover depth revealed that constructing tunnels at deeper depths can mitigate ground surface settlement by fully-mobilized soil-arching.

Table 5 Contact parameters between ball-wall elements

Soil cover depth [mm]	Initial contact force [N]	Final contact force [N]	Height of the loosening zone [mm]
150	15.4	8.8	150
250	24.9	9.24	188
350	33.2	9.38	172

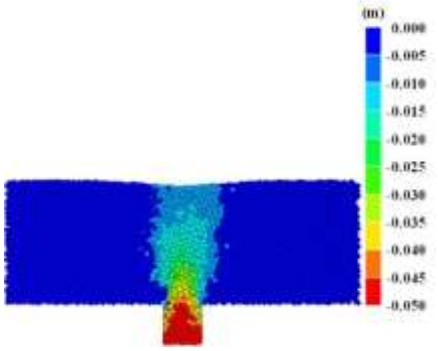

(a) 150 mm

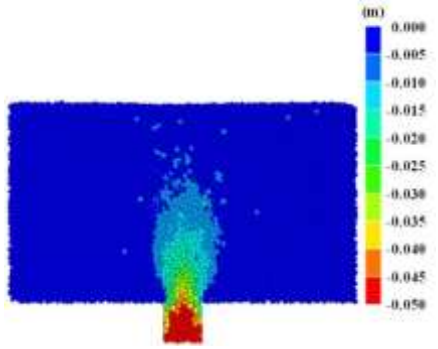

(b) 250 mm

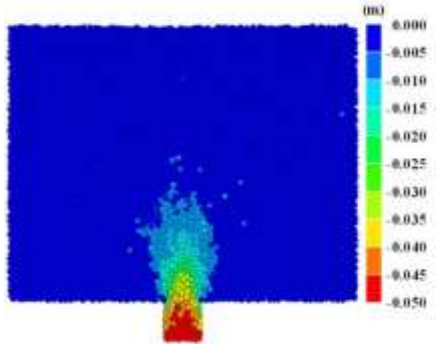

(c) 350 mm

Fig. 12 Particle displacement for each soil cover depth

Further research is essential to comprehensively understand the factors influencing the loosening zone in tunnel design. This investigation should encompass an in-depth analysis of various soil types, particularly those necessitating intricate tunnel designs due to specific ground conditions, such as soft soils and crushed rock masses. Furthermore, it is essential to study tunnel design variables, such as tunnel width and twin tunnel configuration, in the calculation of the loosening earth pressure. The influence of these factors can be assessed by varying the width of the trapdoor plate and exploring a multi-trapdoor configuration.

5. Conclusions

In this study, a DEM-based trapdoor test model was developed to investigate the loosening zone by simulating a NATM tunnel. Using calibrated soil contact parameters, the DEM model can determine the loosening earth pressure and soil particle displacement distribution during the trapdoor test. By considering variations in the soil cover depth, the height of the loosening zone was determined, allowing for the calculation of the loosening earth pressure. The key findings of the numerical simulation are summarized as follows:

- A DEM-based linear contact model was adopted to characterize the behavior of the low-cohesion sand used in the laboratory tests. A numerical model for replicating the triaxial compression test was developed to determine the Mohr-Coulomb strength parameters, and calibrated contact parameters were determined for numerical modeling.
- The DEM model, validated through the laboratory trapdoor test, was applied to describe the behavior of soil particles and estimate the loosening zone. As the trapdoor moved downward, a soil-arcing effect was observed, confirming the redistribution of soil pressure.
- With increasing downward movement of the trapdoor, the loosening zone expanded towards the ground's surface. In cases where ground depth is insufficient, surface settlement may occur. Therefore, a conservative approach is necessary when designing tunnel linings for shallow soil cover depths.
- With greater soil cover depths, the soil-arching effect was reinforced, resulting in increased redistributed contact stress and reduced earth pressure on the trapdoor plate. Moreover, as long as the soil cover depth was sufficient to prevent surface settlement, the loosening zone converged to a specific size with an elliptical shape, which did not grow larger.

Acknowledgments

This research was conducted with the support of the “National R&D Project for Consecutive Excavation Technological Development Project of Tunnel Boring Machine (RS-2022-00144188)” funded by the Korea Agency for Infrastructure Technology Advancement under the Ministry of Land, Infrastructure and Transport, and managed by the Korea University.

References

Chen, R.P., Tang, L.J., Ling, D.S. and Chen, Y.M. (2011), "Face stability analysis of shallow shield tunnels in dry sandy ground using the discrete element method", *Comput. Geotech*,, **38**(2), 187-195. https://doi.org/10.1016/j.compgeo.2010.11.003.

Cho, N., Martin, C.D. and Sego, D.C. (2007), "A clumped particle model for rock", *Int. J. Rock Mech. Min. Sci.*, **44**(7), 997-1010. https://doi.org/10.1016/j.ijrmms.2007.02.002.

Choi, S.W., Lee, H., Choi, H., Chang, S.H., Kang, T.H. and Lee, C. (2020), "Numerical analysis of EPB TBM driving using coupled DEM-FDM Part I: Modeling", *Tunn. Undergr. Sp. Tech.*, **30**(5), 484-495. https://doi.org/10.7474/TUS.2020.30.5.496.

Cundall, P.A. and Strack, O.D.L. (1979), "A discrete numerical model for granular assemblies", *Geotechnique*, **29**(1), 47-65. https://doi.org/10.1680/geot.1979.29.1.47.

Do, T.N., Wu, J.H. and Lin, H.M. (2017), "Investigation of sloped surface subsidence during inclined seam extraction in a jointed rock mass using discontinuous deformation analysis", *Int. J. Geomech.*, **17**(8). https://doi.org/10.1061/(asce)gm.1943-5622.0000894

Fakhimi, A., Carvalho, F., Ishida, T. and Labuz, J.F. (2002), "Simulation of failure around a circular opening in rock", *Int. J. Rock Mech. Min. Sci*., **39**(4), 507-515. https://doi.org/10.1016/S1365-1609(02)00041-2.

Han, J., Wang, F., Al-Naddaf, M. and Xu, C. (2017), "Progressive development of two-dimensional soil arching with displacement", *Int. J. Geomech.*, **17**(12). https://doi.org/10.1061/(asce)gm.1943-5622.0001025.

Hong, W.P. and Kim, H.M. (2014), "A model test on soil arching and loosening zone developed in grounds composed of granular soil particles", *J. Korean Geotech. Soc.*, **30**(8), 13-24. https://doi.org/10.7843/KGS.2014.30.8.13.

Hu, X., He, C., Lai, X., Walton, G., Fu, W. and Fang, Y. (2020), "A DEM-based study of the disturbance in dry sandy ground caused by EPB shield tunneling", *Tunn. Undergr. Sp. Tech.*, **101**. https://doi.org/10.1016/j.tust.2020.103410.

Itasca Consulting Group Inc. (2021), PFC 6.0 Document; Itasca Consulting Group, Minneapolis, MN, USA. https://docs.itascacg.com/pfc600/pfc/docproject/index.html.

Jiang, M. and Yin, Z.Y. (2012), "Analysis of stress redistribution in soil and earth pressure on tunnel lining using the discrete element method", *Tunn. Undergr. Sp. Tech.*, **32**, 251-259. https://doi.org/10.1016/j.tust.2012.06.001.

Jung, J. (2009), "The effect of apparent cohesion of unsaturated soils on behavior of underground structures", Ph.D. Dissertation, Korea University.

Karl, T. (1943), Theoretical Soil Mechanics, John Wiley and Sons, New York

Koutsabeloulis, N.C. and Grifliths, D.V. (1989), "Numerical modelling of the trap door problem", *Geotechnique*, **39**(1), 77-89. https://doi.org/10.1680/geot.1989.39.1.77.

Ladanyi, B. and Hoyaux, B. (1969), "A study of the trap-door problem in a granular mass", *Can. Geotech. J.*, **6**(1), 1-14. https://doi.org/10.1139/t69-001.

Lee, H., Choi, H., Choi, S., Chang, S., Kang, T. and Lee, C. (2021), "Numerical simulation of EPB shield tunnelling with TBM operational condition control using coupled DEM–FDM", *Appl. Sci.*, **11**(6), 2551-2551. https://doi.org/10.3390/app11062551.

Liakas, S., O'Sullivan, C. and Saroglou, C. (2017), "Influence of heterogeneity on rock strength and stiffness using discrete element method and parallel bond model", *J. Rock Mech. Geotech. Eng.*, **9**(4), 575-584. https://doi.org/10.1016/j.jrmge.2017.02.003.

Liang, L., Xu, C., Chen, Q. and Chen, Q. (2020), "Experimental and theoretical investigations on evolution of soil-arching effect in 2D trapdoor problem", *Int. J. Geomech.*, **20**(6). https://doi.org/10.1061/(ASCE)GM.1943-5622.0001643.

McNulty, J.W. (1965), "An experimental study of arching in sand", Ph.D. Dissertation, University of Illinois

Moradi, G. and Abbasnejad, A. (2015), "Experimental and numerical investigation of arching effect in sand using modified Mohr Coulomb", *Geomech. Eng.*, **8**(6), 829-844. https://doi.org/10.12989/gae.2015.8.6.829.

Murayama, S. and Matsuoka, H. (1971), "Earth pressure on tunnels in sandy ground", *Proceedings of the Japan Society of Civil Engineers*, **1971**(187), 95-108. https://doi.org/10.2208/jscej1969.1971.187_95.

Pardo, G.S. and Sáez, E. (2014), "Experimental and numerical study of arching soil effect in coarse sand", *Comput. Geotech.*, **57**, 75-84. https://doi.org/10.1016/j.compgeo.2014.01.005.

Sarfarazi, V. and Tabaroei, A. (2020), "Numerical simulation of the influence of interaction between Qanat and tunnel on the ground settlement", *Geomech. Eng.*, **23**(5), 455-466. https://doi.org/10.12989/gae.2020.23.5.455.

Seo, S.H., Chang, S.B. and Lee, S.D. (2002), "An analysis model of the secondary tunnel lining considering ground-primary support-secondary lining interaction", *Tunn. Undergr. Sp. Tech.*, **12**(2), 107-114.

Shang, J. (2020), "Rupture of veined granite in polyaxial compression: Insights from three-dimensional discrete element method modeling", *J. Geophys. Res.: Solid Earth*, **125**(2). https://doi.org/10.1029/2019JB019052.

Shen, Z., Jiang, M. and Thornton, C. (2016), "DEM simulation of bonded granular material. Part I: Contact model and application to cemented sand", *Comput. Geotech.*, **75**, 192-209. https://doi.org/10.1016/j.compgeo.2016.02.007.

Song, J., Chen, K., Li, P., Zhang, Y. and Sun, C. (2018), "Soil arching in unsaturated soil with different water table", *Granular Matter*, **20**(4). https://doi.org/10.1007/s10035-018-0849-3.

Su, D., Chen, W., Wang, X., Huang, M., Pang, X. and Chen, X. (2022), "Numerical study on transverse deformation characteristics of shield tunnel subject to local soil loosening", *Undergr. Space (China)*, **7**(1), 106-121. https://doi.org/10.1016/j.undsp.2021.07.001.

Tavarez, F.A. and Plesha, M.E. (2007), "Discrete element method for modelling solid and particulate materials", *Int. J. Numer. Method. Eng.*, **70**(4), 379-404. https://doi.org/https://doi.org/10.1002/nme.1881.

Tu, F., Ling, D., Hu, C. and Zhang, R. (2017), "DEM–FEM analysis of soil failure process via the separate edge coupling method", *Int. J. Numer. Anal. Method. Geomech*., **41**(9), 1157-1181. https://doi.org/10.1002/nag.2666.

Wu, J.H., Ohnishi, Y. and Nishiyama, S. (2004), "Simulation of the mechanical behavior of inclined jointed rock masses during tunnel construction using Discontinuous Deformation Analysis (DDA)", *Int. J. Rock Mech. Min. Sci.*, **41**(5), 731-743. https://doi.org/10.1016/j.ijrmms.2004.01.010.

Xu, Z.H., Wang, W.Y., Lin, P., Xiong, Y., Liu, Z.Y. and He, S.J. (2020), "A parameter calibration method for PFC simulation: Development and a case study of limestone", *Geomech. Eng.*, **22**(1), 97-108. https://doi.org/10.12989/gae.2020.22.1.097.

Yang, S.Q., Chen, M., Fang, G., Wang, Y.C., Meng, B., Li, Y.H. and Jing, H.W. (2018), "Physical experiment and numerical modelling of tunnel excavation in slanted upper-soft and lower-hard strata", *Tunn. Undergr. Sp. Tech.*, **82**, 248-264. https://doi.org/10.1016/j.tust.2018.08.049.

Zhao, C., Alimardani Lavasan, A., Barciaga, T., Kämper, C., Mark, P. and Schanz, T. (2017), "Prediction of tunnel lining forces and deformations using analytical and numerical solutions", *Tunn. Undergr. Sp. Tech.*, **64**, 164-176. https://doi.org/10.1016/j.tust.2017.01.015.

Zhou, W., Hou, T., Yang, Y., Niu, Y., Luo, Y. and Yang, C. (2023), "Discrete element numerical simulation of dynamic strength characteristics of expanded polystyrene particles in lightweight soil", *Geomech. Eng.*, **34**(5), 577-595. https://doi.org/10.12989/gae.2023.34.5.577.

Zhu, X., Liu, W. and Lv, Y. (2017), "The investigation of rock cutting simulation based on discrete element method", *Geomech. Eng.*, **13**(6), 977-995. https://doi.org/10.12989/gae.2017.13.6.977.